Journal of Neonatal Surgery
ISSN(Online):2226-0439
Vol.14, Issue 33s (2025)
https://www.jneonatalsurg.com

Tribological Behavior And Surface modification Of FG220 Cast Iron Via CVD Ar–Co_2 Plasma Carburization

Mirza Ateeb Beg Rajvi[1], Dr. Anil Kumar Rao[2]
[1] Research Scholar, Rabindranath Tagore University, Raisen, Madhya Pradesh –462001, India.
Email:ateeb.razvi@gmail.com
[2]Assistant Professor, Rabindranath Tagore University, Raisen, Madhya Pradesh –462001, India.
Email: raoanilkumar2019@gmail.com

Cite this paper as: Mirza Ateeb Beg Rajvi, Dr. Anil Kumar Rao (2025) Tribological Behavior and Surface modification Of FG220 Cast Iron Via CVD Ar–CO_2 Plasma Carburization. Journal of Neonatal Surgery, 14, (33s) 1460-1465

ABSTRACT

This study investigates the tribological performance and surface modification of FG220 grade cast iron that has undergone Ar–CO_2 plasma carburization in conjunction with Chemical Vapour Deposition (CVD). The impact of CO_2 assisted plasma treatment on wettability, sliding wear behaviour, nanoscale roughness, and surface morphology was thoroughly examined. Surface roughness is strongly dependent on the Ar–CO_2 gas flow ratio, according to Atomic Force Microscopy (AFM), with the 10:10 SCCM condition yielding the highest root-mean-square (RMS) roughness of 245 nm. In comparison to the untreated substrate, ball-on-disk tribological tests showed a significant decrease in the coefficient of friction and improved wear resistance after carburisation. The development of a compact, carbon-rich surface layer that encourages stable sliding and lowers material loss is responsible for the enhanced tribological performance. The existence of graphitic and amorphous carbon structures within the wear tracks was verified by Raman spectroscopy investigation, suggesting that the treated surface underwent structural change during sliding. Measurements of the water contact angle also showed that, following plasma treatment, surface wettability significantly changed from hydrophilic behaviour (~57°) to hydrophobic behaviour (>90°). The potential of CO2-assisted CVD carburization as an environmentally friendly surface engineering technique for enhancing the durability and tribological performance of cast iron components in demanding mechanical and industrial applications is demonstrated by the combined effects of controlled surface roughness, carbon-rich layer formation, and modified wettability.

Keywords: FG220 Cast Iron, Chemical Vapor Deposition (CVD), Ar–CO_2 Plasma Carburization,Tribology, Atomic Force Microscopy, Wettability Transition, Amorphous Carbon

1. INTRODUCTION

Flake graphite cast iron, particularly grade FG220, remains an indispensable engineering material across automotive, energy, and industrial manufacturing sectors owing to its excellent castability, high thermal conductivity, and superior vibration damping capacities However, untreated FG220 cast iron suffers from severe inherent mechanical limitations, including low surface hardness, presence of surface-connected porosity, heterogeneous distribution of graphite flakes, and extreme susceptibility to adhesive wear, abrasion, and aggressive environmental corrosion under un lubricated sliding conditions.

To mitigate these mechanical shortcomings, advanced surface modification techniques have gained widespread attention. Among these, Diamond-Like Carbon (DLC) and carbonaceous thin films synthesized via Chemical Vapor Deposition (CVD) provide an exceptionally dense, chemically bonded protective boundary characterized by high hardness, low chemical reactivity, and ultra-low friction coefficients. Unlike conventional surface treatments or line-of-sight thermal spray methods, plasma-assisted CVD ensures uniform, conformal coverage across complex mechanical geometries with robust film-substrate adhesion. Recent advancements emphasize the integration of eco-friendly reactive gases specifically carbon dioxide (CO_2) in plasma systems.CO_2-assisted CVD plasma carburization not only facilitates controlled carbon atom diffusion into the iron matrix but also provides a sustainable framework for CO_2 utilization in industrial surface processing. Numerous prior studies have investigated various surface engineering strategies on metallic alloys. Sharma et al. (2024) reported significant reductions in the coefficient of friction (COF) using multilayer grapheme and WS_2. Çelik et al. (2004) and Marcinauskaset al. (2024) examined plasma-sprayed nickel-graphite and alumina coatings on steel, demonstrating that controlled graphite fractions reduce sliding friction Spin-coated MAX-phase and composite carbon coatings achieved up to 82% friction reduction. (Bharti, Neogi, etal.,2024), whereas high mechanical loads on tool steel highlighted complex shear dynamics in dense graphite layers.

(Bharti, Jaiswal, etal.,2024) Furthermore, plasma carburizing and PECVD amorphous carbon (a-C:H) depositions on titanium alloys (Ti6Al4V) and stainless steels have consistently proven effective in suppressing creep, altering surface energy and enhancing corrosion resistance (De Oliveira et al., 2015; Zhang et al., 2023; Almeida et al., 2020). Building upon these insights, this study provides a comprehensive investigation into the effect of varying Ar–CO_2 gas flow ratios during CVD plasma carburization on the surface roughness, wettability, structural ordering, and tribological performance of FG220 cast iron.

2. EXPERIMENTALMATERIALS&METHODS

2.1 Substrate Preparation

Substrates of FG220 grade cast iron were prepared in square dimensions of 10 cm × 10 cm with a thickness of 5 mm. To establish a standardized surface condition prior to plasma treatment, the substrates were ground and polished using silicon carbide (SiC) emery papers with progressive grit sizes from 80 to 2000. Following mechanical polishing, the samples underwent sequential multi-stage ultrasonic cleaning in acetone, isopropyl alcohol (IPA), and deionized (DI) water for 10 minutes per stage at room temperature. This rigorous cleaning protocol ensured complete removal of organic contaminants, abrasive particulates, and surface oxides.

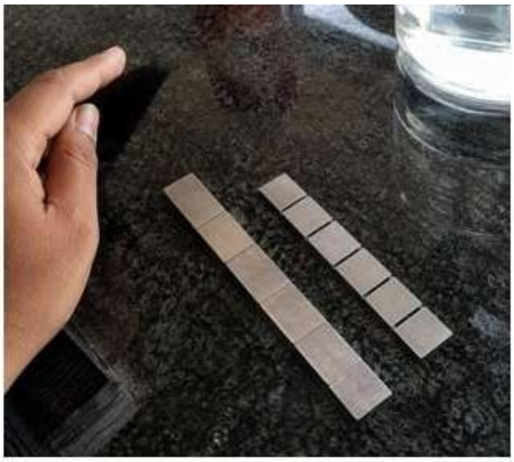

Figure 1 - Sample Preparation.

Figure 2 - Ultrasonic cleaning of polished sample.

Table1: Substrate specifications and operational parameters for CVD Ar–CO_2 plasma treatment.

PARAMETER CATEGORY	SPECIFICATION/OPERATIONAL CONDITION
Substrate Material & Grade	CastIron, GradeFG220 (Flake Graphite)
Substrate Dimensions	100mm×100mm×5mm (Square Plate)
Pre-Treatment Cleaning	Ultrasonic bath in Acetone →IPA→DI Water(10mineach)
CVD Chamber Base	Pressure10−3mbar
In-Situ Plasma Etching	Pure Argon (Ar) at 0.26mbar,60WRFBias
Process Operating Pressure	10−2 mbar (VacuumValvetunedto25%)
Gas Mixtures (Ar: CO_2)	10:10SCCM,10:20SCCM, and10:30SCCM
Gas Purities	Argon (99.99%), Carbon Dioxide (99.98%)
RF Power Bias & Duration	60WRF Bias; Treatment time:1hrand5 hr

2.2 CVD Plasma Carburization Protocol

The carburization process was conducted in a custom Radio Frequency (RF) Chemical Vapor Deposition chamber. Substrates were placed on the cathode assembly, and the chamber was evacuated to a base pressure of 10−3 mbar. In-situ plasma etching was initially performed under pure Argon gas flow at 0.26 mbar with an applied RF bias of 60 W to sputter clean residual native oxides.

Subsequently, the vacuum valve position was set to 25% to stabilize the operating pressure at 10−2 mbar. High-purity Ar (99.99%) at a constant rate of 10 SCCM and high-purity CO_2 (99.98%) at varying flow rates (10, 20, and 30 SCCM) were introduced via calibrated Mass Flow Controllers (MFC) Carburization was driven by maintaining a 60 W RF plasma bias for durations of 1 hour and 5 hours.

Figure 3 - CVD process of DLC Deposition for FG 220

2.3 Surface Characterization Techniques

Surface topographical evolution and nano-scale roughness were measured using Atomic Force Microscopy (AFM) operated in tapping mode across scan areas of 5 µm × 5 µm Surface parameters including Root-Mean- Square Roughness (Rq) and Average Roughness (Sa) were computed.The tribological performance was evaluated using a ball-on-disk tribometer under un lubricated dry sliding conditions at 24 °C and 48% relative humidity. A hardened steel ball of 2 mm diameter was loaded at 1.05 N under a constant sliding speed of 1.05 cm/s for 3600 seconds. Post-test wear track profiles and widths were evaluated using optical microscopy at 10X magnification. Phase identification and structural disorder of carbon species inside wear tracks were analyzed using micro-Raman spectroscopy across 1000–2000 cm^{-1}. Surface wettability was quantified via sessile DI water droplet contact angle goniometry under ambient conditions.

3. RESULTS & DISCUSSION

3.1 Atomic Force Microscopy (AFM) & Surface Topography

AFM 3D topographical scans revealed profound changes in surface texture as a function of Ar–CO_2 gas flow ratios.The untreated bare FG220 cast iron exhibited a baseline roughness of Sa = 10.98 nm. Upon Ar–CO_2 plasma exposure, significant nano scale hillock growth and inter phase nucleation occurred.

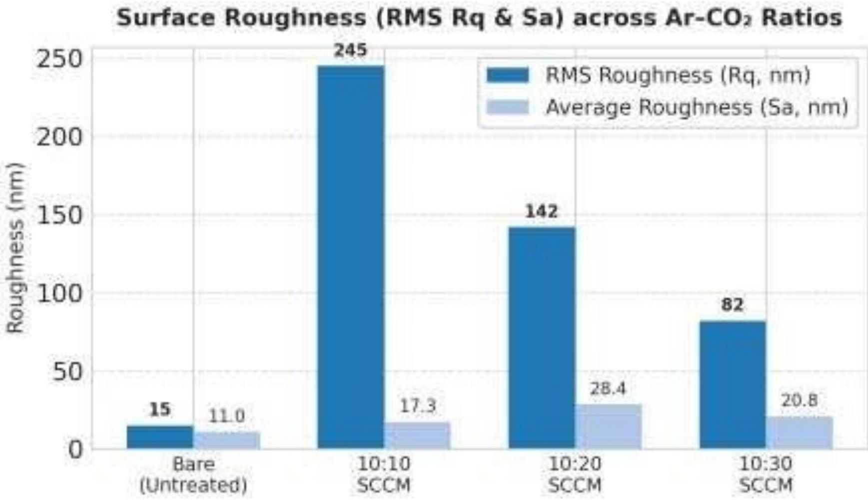

Graph 1: Evolution of surface roughness parameters (RMS Rq and Sa) across untreated and Ar–CO_2 plasma carburized FG220 cast iron substrates

As summarized in Graph 1, the 10:10 SCCM Ar–CO_2 condition produced the highest RMS surface roughness (Rq = 245 nm; Sa = 17.29 nm). Increasing the CO_2 flow rate to 10:20 SCCM and 10:30 SCCM led to a progressive decline in RMS roughness to 142 nm (Sa = 28.44 nm) and 82 nm (Sa = 20.78 nm), respectively.
At equal gas ratios (10:10 SCCM), optimal plasma dissociation promotes energetic carbon species flux and aggressive ion etching, enhancing atomic diffusion into the cast iron matrix and forming a highly textured, carburized inter phase. Higher CO_2 concentrations introduce excess oxygen species in the plasma discharge, which induce competitive chemical etching and oxidation of growing carbon clusters, thereby smoothing the outer layer topography.

3.2 Tribological Behavior & Wear Track Analysis

The coefficient of friction (COF) vs. sliding time curves and post-test wear track widths are illustrated in Graph 2. Untreated FG220 cast iron exhibited a rapid rise in COF during the running-in phase, reaching a steady-state value of ~0.50 with pronounced frictional fluctuations caused by adhesive wear, severe plastic deformation, and debris accumulation.

Conversely, plasma-carburized samples demonstrated a substantial reduction in COF and a highly stable sliding response under normal loading (1 N), the hard, modified carbonaceous diffusion layer resisted penetration by the steel counter body The wear track width on the untreated sample was measured at 438.0 µm. Plasma carburization significantly narrowed the wear scar dimensions: 353.84 µm for 10:10 SCCM, 376.80 µm for 10:20 SCCM, and 386.84 µm for 10:30 SCCM.The superior wear resistance of the 10:10 SCCM condition stems from the formation of a dense, thick carburized zone possessing high shear strength, which limits true contact area and provides solid lubrication during sliding.

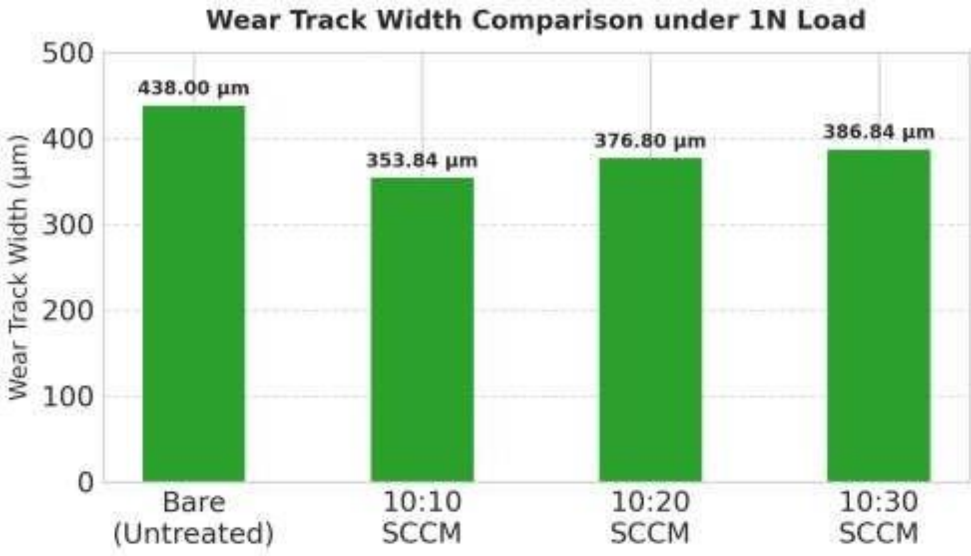

Graph 2: Comparative weartrackwidthsformedonuntreatedandplasmacarburizedFG220cast ironafter3600s dry sliding against a steel counter body

3.3 Raman Spectroscopy Analysis

Raman spectra recorded within the wear tracks of carburized samples revealed broad, asymmetric scattering bands spanning 1000 cm^{-1} to 2000 cm^{-1} Spectral deconvolution confirmed the presence of characteristic carbonaceous resonance features, namely the disordered D-band (~1350 cm^{-1}) associated with SP^3 breathing modes and the graphitic G-band (~1580 cm^{-1}) corresponding to in-plane stretching of SP^2 carbon pairs. The presence of these prominent broad peaks confirms the synthesis of an amorphous carbonaceous structure containing embedded graphitic domains. During mechanical contact, this amorphous carbon layer shears easily under tangential forces, providing a low-shear interfacial transfer film that suppresses direct metal-to-metal contact and mitigates wear.

3.4 Surface Wettability Transition

Wettability analysis demonstrated a marked shift in surface free energy and chemical affinity following Ar–CO_2 plasma treatment. As shown in graph 3, the untreated FG220 cast iron substrate exhibited hydrophilic behavior with a native water contact angle of ~57° due to high surface energy and polar iron oxide bonds.

Following CVD plasma carburization, all treated surfaces transitioned into a distinct hydrophobic state, recording water contact angles well above 90° (peaking at ~105° for the 10:10 SCCM condition) This hydrophobicity is attributed to the combined effects of hierarchical nanoscale roughness induced by ion sputtering (as verified by AFM) and the passivation of polar surface sites by non-polar carbonaceous (C–C / C–H) functional groups. This hydrophobic conversion offers critical benefits for industrial components, offering enhanced resistance to aqueous corrosion and liquid adhesion.

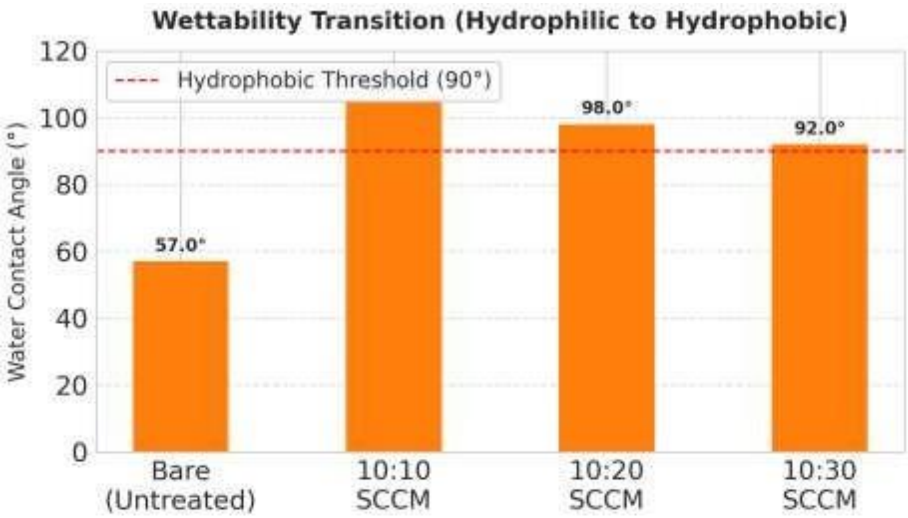

Graph 3: Water contact angle transformation showing the shift from hydrophilic native castiron (~57°) to hydrophobic states (>90°) post carburization

4. CONCLUSION

This study successfully demonstrated the efficacy of Ar–CO_2 plasma carburization via RF Chemical Vapor Deposition for tailoring the surface and tribological properties of FG220 grade cast iron. The main findings are summarized below:

- **Topographical Tuning:** Gas flow ratios strongly influence surface roughness. The 10:10 SCCM Ar–CO_2 ratio generated the highest RMS surface roughness (245 nm), establishing a dense, highly textured interphase layer.
- **Tribological Superiority**: Carburized substrates achieved significant friction reduction and improved wear resistance compared to untreated cast iron. The 10:10 SCCM treatment yielded the narrowest wear track width (353.84 µm vs. 438.0 µm for untreated).
- **Structural Phase Synthesis**: Raman spectroscopy confirmed the formation of amorphous carbonaceous structures containing embedded graphitic SP^2 domains within the wear track, providing self-lubricating transfer film characteristics.
- **Wettability Reversal**: Plasma treatment transformed the native hydrophilic cast iron surface (~57°) into a hydrophobic surface (>90°), enhancing environmental degradation resistance.

Overall, CO_2-assisted CVD plasma carburization represents a highly effective, environmentally sustainable pathway for extending the operational lifespan of cast iron components in demanding mechanical and automotive engineering applications.

REFERENCES

[1] Abe, A., Goss, J. A., & Zou, M. (2024). Exploring the Impact of Spray Process Parameters on Graphite Coatings: Morphology, Thickness, and Tribological Properties. Coatings, 14(6), 714

[2] Bharti, P., Jaiswal, S., Kumar, R., et al. (2024). Large control of friction and wear enabled by Ti3AlC2 MAX-multilayer graphenepolydopamine composites. FlatChem, 46, 100671

[3] Bharti, P., Neogi, A., Sharma, R., et al. (2024). Decision trees within 1D/2D material systems for enabling highly lubricious and wear resistant surfaces. Carbon, 217, 118603

[4] Çelik, E., Tekmen, Ç., & Türk, A. (2004). The fabrication of nickel-graphite coatings on mild steel using plasma-spray techniques. Key Engineering Materials, 264–268, 473–476

[5] De Oliveira, V. M. C. A., Da Silva, M. C. L., et al. (2015). Short-term creep properties of Ti-6Al-4V alloy subjected to surface plasma carburizing process. Journal of Materials Research and Technology, 4(4), 359–366

[6] Marcinauskas, L., Ratautaitė, K., et al. (2024). Influence of Graphite and Zirconia Addition on the Tribological Properties of Plasma-Sprayed Alumina Coatings. Coatings, 14(8), 978

[7] Morstein, C. E., & Dienwiebel, M. (2021). Graphite lubrication mechanisms under high mechanical load. Wear, 477, 203794

[8] Sharma, R., Bharti, P., Jaiswal, S., et al. (2024). A new insight into the contact sliding and wear resistance of 2D/layered materials and their composites based on WS2 and multilayer graphene. Colloids and Surfaces A, 690, 133659

[9] Zhang, H., Zhang, S., Zhang, M., & An, J. (2023). Carburizing of Ti–6Al–4V alloy: Structure, growth mechanism and wear performance. Journal of Materials Research and Technology, 27, 7059–7071

[10] Subash Acharya and Hemantha Kumar. Investigation of magnetorheological brake with rotor of combined magnetic and non-magnetic materials. SN Applied Sciences, 1, 9 2019.

[11] Sambhaji Shivaji Ahirrao, Swapnil Jayesh Ahire, and Sachin Rajendra Bhalerao.A review on drum brakes. www.irjmets.com @International Research Journal of Mod-ernization in Engineering, 661.

[12] K. Ait-Hamouda, A. Ababou, M. Ouchabane, N. Gabouze, S. Belhousse, H. Menari, and K. Beldjilali. Study of optical properties of diamond-like carbon/porous silicon antire-flective coating layers for multicrystalline silicon solar cell applications. Vacuum, 81(11):1472–1475, 2007. Proceed-ings of the selected presentations from Sixth Iberian Vac-uum Meeting and Fourth European Topical Conference on Hard Coatings.

[13] Oluwaseyi Ayodele Ajibade, Johnson Olumuyiwa Agunsoye, and Sunday Ayoola Oke. A wear rate model incorporating inflationary cost of agro-waste filled composites for brake pad applications to lower composite cost. SN Applied Sci-ences, 3, 1 2021.

[14] Ibrahim Alaefour, Samaneh Shahgaldi, Jian Zhao, and Xianguo Li. Synthesis and ex-situ characterizations of diamond-like carbon coatings for metallic bipolar plates in pem fuel cells. International Journal of Hydrogen Energy, 46(19):11059–11070, 2021. Fuel cell and hydrogen energy technology.

[15] D. S. Antunes, D. Masotti, N. F. Ferreira, P. D. Neis, Let´ıcia F.F. Miguel, and J. Favero. Damping effect on non-linear drum brake squeal prediction. Journal of the Brazilian Society of Mechanical Sciences and Engineering, 44, 3 2022.

[16] IK Adi Atmika, IDG Ary Subagia, IW Surata, and IN Su-tantra. Study of mechanical and physical properties of natural hybrid composites. Int. J. Mater. Mech. Manuf., 7:6, 2019.

[17] Siti Nor Nadirah Baba, Muhammad Najib Abdul Hamid, Shahril Nizam Mohamed Soid, Mohd Nurhidayat Zahelem, and Mohd Suyerdi Omar. Analysis of drum brake system for improvement of braking performance. Engineering Applica-tions for New Materials and Technologies, pages 345–357, 2018.

[18] D.C. Barton. Modelling of materials for automotive braking. International Materials Reviews, 49(6):379–385, 2004.

[19] Ali Belhocine and Oday Ibraheem Abdullah and. Finite element analysis (fea) of frictional contact phenomenon on vehicle braking system. Mechanics Based Design of Struc-tures and Machines, 50(9):2961–2996, 2022.